

X-Transfer: A Transfer Learning-Based Framework for Robust GAN-Generated Fake Image Detection

Lei Zhang^{1,*}, Hao Chen^{1,*}, Shu Hu², Bin Zhu³, Xi Wu¹, Jinrong Hu^{1,†}, Xin Wang^{4,†}

¹ Chengdu University of Information Technology

² Indiana University–Purdue University Indianapolis

³ Microsoft Research Asia

⁴ University at Albany, State University of New York (SUNY)

Abstract

Generative adversarial networks (GANs) have remarkably advanced in diverse domains, especially image generation and editing. However, the misuse of GANs for generating deceptive images raises significant security concerns, including face replacement and fake accounts, which have gained widespread attention. Consequently, there is an urgent need for effective detection methods to distinguish between real and fake images. Some of the current research centers around the application of transfer learning. Nevertheless, it encounters challenges such as knowledge forgetting from the original dataset and inadequate performance when dealing with imbalanced data during training. To alleviate the above issues, this paper introduces a novel GAN-generated image detection algorithm called X-Transfer. This model enhances transfer learning by utilizing two sibling neural networks that employ interleaved parallel gradient transmission. This approach also effectively mitigates the problem of excessive knowledge forgetting. In addition, we combine AUC loss term and cross-entropy loss to enhance the model's performance comprehensively. The AUC loss approximates the AUC metric using WMW statistics, ensuring differentiability and improving the performance of traditional AUC evaluation. We carry out comprehensive experiments on multiple facial image datasets. The results show that our model outperforms the general transferring approach, and the best accuracy achieves 99.04%, which is increased by approximately 10%. Furthermore, we demonstrate excellent performance on non-face datasets, validating its generality and broader application prospects.

1 Introduction

Generative Adversarial Networks (Goodfellow et al. 2014) have demonstrated their immense potential in computer vision, particularly image generation. GAN-generated images possess a remarkable level of realism, making it quite challenging to discern them from real ones. This poses a significant concern as GAN-generated images can be exploited for creating fake accounts and various malicious activities. Many tools are available for generating fake images, making it effortless to propagate false information. An illustrative instance is DeepNude (BURGESS 2021), an open-source DeepFake software initially introduced in 2017 and



Figure 1: Fake images generated by StyleGAN2 (Karras et al. 2020).

launched as a website in 2019. The software facilitates transforming one person's face into another's image and changes in body details. Adversaries have used these tools for malicious purposes, posing severe social, security, and ethical concerns. Detecting fake images generated by GANs is of immense importance, leading to the development of numerous detection methods to counteract the misuse of such images. However, existing detection methods still fall short of the expected performance. Detection of GAN-generated images is a complex and challenging task.

In media forensics, earlier studies primarily relied on traditional methods such as SVM, Logistic Regression, and Naive Bayes (Cortes and Vapnik 1995; Cox 1958; Duda, Hart et al. 1973). With the advancement of the feature extraction power and recognition capability of convolutional neural networks (CNNs) (Krizhevsky, Sutskever, and Hinton 2012; Simonyan and Zisserman 2014), an increasing number of researchers have shifted towards using CNN-based methods as their primary approach for feature extraction. As a result, traditional methods have gradually become less prominent in this domain. Many recent studies employ CNNs to determine whether an image is generated by a GAN. Some have demonstrated high detection performance, which can be used to analyze the artifacts or features of GANs (Yang, Li, and Lyu 2019; Mo, Chen, and Luo 2018a; Do, Na, and Kim 2018; Chen et al. 2021).

However, some specific methods exhibit impressive performance only when tested on the dataset they were trained on. These methods often experience a decline in performance when confronted with new and unfamiliar datasets. For example, the model proposed by Bayar's (Bayar and Stamm 2016) exhibits strong performance in detecting image manipulations like median filtering, interpolation, and Gaussian filtering by constraining the initial convolutional

*Equal contribution

†Corresponding author

layer of the CNNs. Although it attains high scores on these manipulations, its performance falters when applied to distinct GAN domains. This showcases good results on the source dataset but struggles on the target dataset. To address this issue, some studies have employed transfer learning (Li et al. 2018; Jeon et al. 2020; Cozzolino et al. 2018). However, directly applying transfer learning methods often leads to discrepancies in performance metrics between datasets. A model may demonstrate superior performance before transfer but experience a decline in performance after the transfer. Conversely, a model may exhibit inferior performance before transfer but showcase improvement post-transfer.

In this paper, we aim to keep a high performance during transfer learning on both the source and target datasets without excessive knowledge forgetting problems. It is taking inspiration from the Hybrid Gradient Forward (Song et al. 2021) and T-GD (Jeon et al. 2020) approaches; we design a sibling structure to carry out transfer learning. This approach involves guiding a master network to learn a new dataset concerning the auxiliary network, effectively preserving the knowledge acquired from the source dataset. The auxiliary network contributes to retaining its sibling’s familiarity with the original dataset while facilitating adaptation to new information during the transfer phase. This ensures the transfer of crucial knowledge from the source dataset to the target dataset, thereby minimizing the risk of significant loss of prior knowledge.

Therefore, we summarize the main contributions of this paper as follows:

1. We employ a novel transfer learning framework to enhance the overall detection performance of the model. Our objective is to maintain a high level of discrimination performance between these two distinct datasets throughout the transfer learning process while mitigating the issue of excessive knowledge forgetting.
2. We introduce an algorithm including two same architecture networks named *X-Transfer*. It achieves guaranteed before and after transfer learning performance by balancing between hybrid gradient passes as well as network iterations. We also employed the WMW-AUC loss, which can enhance the detection performance in general.

This paper is organized as follows. Section *Related work* summarizes the related works on GAN-generated face detection. Section *Methodology* mainly depicts our GAN-generated image detection method, including X-Transfer and AUC Loss. Section *Experiments* indicates experimental results. Section *Conclusion* concludes our work.

2 Related Work

Detection of GAN-generated Images

With the powerful capabilities of Convolutional Neural Networks (CNNs), the most recent detection methods utilize deep learning methods.

Mo et al. (Mo, Chen, and Luo 2018b) proposed the first CNN-based detection method that focuses on high-frequency components to detect face images generated by Progressive Growing GAN (PGGAN) (Karras et al. 2017),

achieving impressive performance. They applied a high-pass filter to preprocess an image before inputting it into the CNN, further improving the detection accuracy. However, this method is fragile when faced with image compression and blurs. Nataraj et al. (Nataraj et al. 2019) proposed a method that combines co-occurrence matrices and JPEG compression as a tactic for data augmentation. Co-occurrence matrices are extracted from the RGB channels of the input image, then stacked according to the channel dimensions, and finally input into a shallow CNN (such as ResNet-18) to obtain the final detection result. In addition to co-occurrence matrices, researchers have considered introducing preprocessing methods from other traditional forensic techniques into GAN-generated image detection. Mi et al. (Mi et al. 2020) introduced a detection approach employing the self-attention mechanism. This mechanism effectively expands the perception field of convolutional neural networks, enhancing their ability to extract and represent global information. In addition to extracting multiple up-sampling information from GAN more efficiently, it alleviates the spatial distance problem encountered by traditional convolutional neural networks. Their experimental results demonstrate that this method can proficiently identify images generated by PGGAN and exhibits robustness against common post-processing operations.

Data Augmentation for post-processing operation

One of the challenges in practical applications of image detection generated by GAN is the interference of post-processing operations. Post-processing operations refer to a series of image or data manipulation steps applied after an initial process, such as resizing, scaling, compression, and filtering. These post-processing operations may degrade the recognition performance of the model. Wang et al. (Wang et al. 2020) introduced data augmentation methods into their GAN-generated image detection to make a detection method robust to post-processing operations. The authors used ResNet-50 (He et al. 2016) as the backbone and PGGAN-generated images as the training set. They considered five different data augmentation methods: no data augmentation, Gaussian blur, JPEG compression, Gaussian blur, and JPEG compression with a 50% probability, and Gaussian blur and JPEG compression with a 10% probability. Before inputting into the model, samples were cropped and randomly flipped. Their results indicate that data augmentation can enhance the robustness of GAN-generated image detection models when faced with post-processing operations. It can also increase the diversity of training samples and improve detection performance.

In addition to commonly used random rotation, JPEG compression, and Gaussian filtering that researchers have applied before, we also used CutMix (Yun et al. 2019), random JPEG compression and AlignMixup (Venkataramanan et al. 2022).

Transfer Learning

Transfer learning has been widely used in GAN-generated image detection. Hyeonseong et al. (Jeon et al. 2020) employed a neural network based on a teacher-student model,

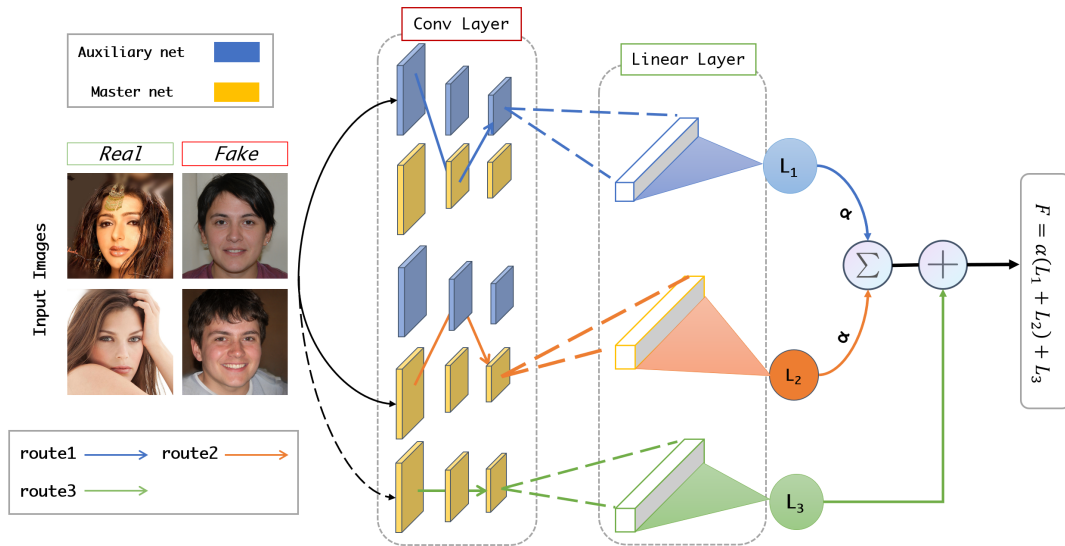


Figure 2: The Structure of the X-Transfer Algorithm is depicted as follows. Initially, we train an original neural network using the source dataset. Subsequently, we transfer its parameters into sibling networks with the same architecture, comprising an auxiliary network and a master network. To ensure that the master network retains its knowledge, we freeze the weights of the auxiliary network and focus on training the master network using the target dataset. Different transmission routes yield distinct losses when cross-entropy calculations are performed between the two networks. These cross-entropy losses are harmonized and amalgamated with the AUC loss and L2 regularization function. This amalgamation elevates the overall AUC score, resulting in enhanced performance, even in scenarios involving imbalanced datasets, while mitigating the risk of excessive knowledge degradation.

transfer learning, and regularization function. They used a pre-trained network as the teacher model and a starting reference for the student through an L_2 regularization function to restrict the variation of convolutional layers between the teacher and student networks, minimizing excessive knowledge forgetting during transfer learning.

Our method differs in utilizing a mixed gradient propagation approach between two networks for each of their corresponding sub-layers. This approach assists in preventing excessive knowledge forgetting and facilitates knowledge acquisition.

3 Methodology

Overview

Our research endeavors to tackle the issue of declining performance observed in the original model during the transfer learning process. The architectural framework of our algorithm is visually depicted in Figure 2. Fundamentally, this framework comprises two integral parts: a master and an auxiliary network. These components mirror each other’s structure and originate from the same model. However, the sibling networks work in tandem to update weights through separate routes during the transfer learning process. Input data is propagating through alternating sub-networks of the auxiliary network and master network. More precisely, the forward pass transitions to the other network just before reaching the downsampling layer. This approach is rooted in the convention that feature maps preceding the downsam-

pling layer are often valuable for task-specific predictions. In other words, the feature map extracted immediately before downsampling provides a strong representation of that particular image scale. Using alternating fashion can avoid overfitting when absorbing knowledge during transferring.

As depicted in Figure 2, we define two routes stemming from the sibling network. The first route, starting from the auxiliary network, is referred to as “**route1**”, and its corresponding loss is labeled as L_1 . Conversely, the second route, emanating from the master network, is named “**route2**”, with its associated loss indicated as L_2 . Additionally, the output directly produced by the master model is represented as L_3 , and its route is termed “**route3**.” Our primary objective is to strike a harmonious balance among these losses while preserving the prior knowledge acquired during the pre-training phase. For this purpose, we introduce the “X-Transfer” algorithm, which will be elaborated upon in Section *X-Transfer*.

In addition, we consider that the imbalanced training data would cause the typical evaluation metrics (e.g., accuracy) to be biased by most class samples. We adopt the **Wilcoxon-Mann-Whitney (WMW)** statistic to simulate the AUC loss function in combination with the binary cross-entropy loss. Through experimental verification, we find that incorporating the AUC Loss yields improved model performance. This highlights the effectiveness of the AUC Loss in training a model that can handle imbalanced datasets more effectively and achieve higher AUC scores.

X-Transfer

As previously mentioned, our proposed method, ‘‘X-Transfer,’’ which is phonetically similar to ‘‘Crossed Transfer,’’ primarily comprises two neural networks, a master network and an auxiliary network, originating from the same source model. Throughout the training process, three distinct routes will be executed and are explained as follows.

Route 1. This route starts with the auxiliary network; the feedforward passes the training data through a sub-network of layers of the master network and then a sub-network of an auxiliary network alternately, while the back-propagation only updates the layers involved in the feed-forward process and leaves the others fixed. We denoted the loss as L_1 .

Route 2. Just like *Route 1*, with the distinction that this route originates from the master network. During the feedforward phase, the training data is sent through sub-networks within both the master and auxiliary networks alternately. However, during back-propagation, updates are exclusively applied to the layers participating in the feedforward process, while the remaining layers remain unchanged. We’ve designated the resulting loss as L_2 .

Route 3. Differing from the previous routes, this particular route distinguishes itself in terms of loss propagation. It commences from the master neural network only and propagates data directly through all the layers of the master network sequentially without branching into distinct sub-layers of the auxiliary network. We refer to this cross-entropy loss as L_3 .

Our target is to balance the multi-losses above three routes and finally retrieve the transferred model of the master network. Let $\{(x_i, y_i)\}_{i=1}^M$ be a mini-batch of target dataset where x_i represents the i th data and y_i is the true label for x_i , M stands for the size of mini-batch. In a mini-batch, L_1, L_2, L_3 are the cross-entropy losses we described. Each of them can be calculated by $\frac{1}{M} \sum_{i=1}^M J(y_i, \hat{y}_i)$, where J is the cross-entropy loss function and $\hat{y}_i = f(x_i)$. $f(x_i)$ is the output of the neural network function, and three routes have different $f(x_i)$ output.

Let F be the combination function of L_1, L_2 , and L_3 , and it mainly controls the weights of these losses. Our overall loss function is depicted in the equation (1):

$$L = F(L_1, L_2, L_3) \quad (1)$$

During the transferring stage, we hope that the master network can maintain the expected detection performance of the original dataset while learning from the knowledge of the target dataset without excessively forgetting the source dataset. For each training mini-batch, the final loss is $F = \alpha(L_1 + L_2) + L_3$. Denoting the neural network’s training weights as ω , the gradient expression for the backpropagation about F is depicted in equation (2).

$$\frac{\partial F}{\partial \omega} = \alpha \cdot \left(\frac{\partial L_1}{\partial \omega} + \frac{\partial L_2}{\partial \omega} \right) + \frac{\partial L_3}{\partial \omega} \quad (2)$$

Here, we introduce α to restrict the magnitudes of L_1 and L_2 , preventing them from becoming excessively large and interfering with the network’s ability to fit the target dataset

Algorithm 1: X-Transfer Algorithm

Input: $\{(x_i, y_i)\}_{i=1}^N$ with data size N , a dataset of real and generated images and their labels

Input: Pre-trained model: auxiliary network \mathbf{f} and master network \mathbf{g}

Hyperparameters: $s > 0, \beta \in (0, 1), B > 0$

- 1: **X-Net:** the composition of sibling network for X-Transfer
 - 2: $m \in \{0, 1\}$ is a constant ▷ Control the entrance of X-Net
 - 3: **for** $k \in \{1, 2, \dots, \frac{N}{B}\}$ **do** ▷ Batch iterations
 - 4: $\{L_1, L_2, L_3, L_{AUC}, \alpha\} = 0$ ▷ Initialize sums
 - 5: $\{X, Y\} = \{(x_j, y_j)\}_{j=1}^B$ ▷ Get next batch
 - 6: $Out_1 = \mathbf{X-Net}(\{X|m=0\})$ ▷ forward loss start from auxiliary net
 - 7: $Out_2 = \mathbf{X-Net}(\{X|m=1\})$ ▷ forward loss start from master net
 - 8: $Out_3 = \mathbf{g}(X)$ ▷ output of master network
 - 9: $\{L_1, L_2\} = \text{CrossEntropy}(\{Out_1, Out_2\}, \{Y\})$
 - 10: $L_3 = \text{CrossEntropy}(\{Out_3\}, \{Y\})$
 - 11: $L_{AUC} = \text{AUC}(\{Out_3\}, \{Y\})$ ▷ AUC Loss
 - 12: $\alpha = 2 \cdot L_3 / (L_1 + L_2)$
 - 13: $Loss_{main} = \beta \cdot L_3 + (1 - \beta) \cdot L_{AUC}$
 - 14: **Target Loss** $= \alpha \cdot (L_1 + L_2) + Loss_{main} + s \cdot \Omega_{fc}(\omega)$
 - 15: Update the master network \mathbf{g} and minimize the Target Loss for this batch.
 - 16: **end for**
-

properly. Simultaneously, we leverage L_1 and L_2 to maintain the detection performance of the original domain and guard against catastrophic forgetting. According to (Song et al. 2021), the balancing parameter α for each mini-batch j can be calculated by equation (3),

$$\alpha = \frac{2L_3^j}{L_1^j + L_2^j}, \quad (3)$$

where L_1^j, L_2^j , and L_3^j are the L_1, L_2 , and L_3 losses at the j -th mini-batch, respectively. α is initialized with 0. We provide pseudo-code for this algorithm in Alg. 1.

AUC For Improving Imbalanced Learning

In machine learning, we often use accuracy, F1 score, recall, and AUC as the evaluation criteria for classification effect, and most of them can acquire a good performance on the balanced dataset. However, when our dataset is an imbalanced dataset, the metrics above may need to be more effective. Accuracy is less favorable than before since the necessity of the threshold should be set in advance. Compared with accuracy, F1, and recall, AUC and logits-loss are better metric choices when faced with imbalanced datasets. The threshold is unnecessary for both of them. In this work, we choose AUC as our evaluation metric, and we aim to directly maximize the AUC metric to maintain the model’s performance.

AUC metric can measure a model’s performance on a binary classification problem. However, we cannot directly employ the AUC metric in our loss function because it is

nondifferentiable. To maximize the AUC metric, we can use another target loss term to get close to it: the normalized wilcoxon-mann-whitney (WMW) statistic that can simulate AUC and is differentiable.

Given a labeled dataset $\{(x_i, y_i)\}_{i=1}^M$ with M samples, x is the input data and y is its label ($y \in \{0, 1\}$). Then we define two different sets as $P = \{i | y_i = 1\}$, and $N = \{i | y_i = 0\}$. P is the set of positive samples' index, while N is the negative samples' index. Let $\mathcal{F} : \mathbb{R}^d \rightarrow \mathbb{R}$, \mathcal{F} is a predict function that maps a d -dimensional tensor to a one-dimensional real number space. $\mathcal{F}(x_i)$ represents the predication score of sample x_i , where $i \in [1, M]$.

According to Wilcoxon Mann Whitney statistics (WMW) (Yan et al. 2003), we can get an approximate AUC loss as follows:

$$L_{AUC} = \frac{1}{|P||N|} \sum_{i \in P} \sum_{j \in N} R(\mathcal{F}(x_i), \mathcal{F}(x_j)), \quad (4)$$

$$R(\mathcal{F}(x_i), \mathcal{F}(x_j)) = \begin{cases} -(\mathcal{F}(x_i) - \mathcal{F}(x_j) - \gamma))^p, & \text{otherwise} \\ 0, & \mathcal{F}(x_i) - \mathcal{F}(x_j) \geq \gamma \end{cases}, \quad (5)$$

where $\gamma \in (0, 1]$ and $p > 1$ are two hyper-parameters. We set γ as 0.16 and p as 2 in this experiment.

Total loss of our method Finally, we define a hyper-parameter $\beta \in [0, 1]$ to balance the binary cross-entropy(BCE) loss function and AUC loss function L_{AUC} , the target equation are shown as below:

$$L = \alpha \cdot (L_1 + L_2) + \beta \cdot L_3 + (1 - \beta)L_{AUC} + s \cdot \Omega_{fc}(\omega), \quad (6)$$

where Ω_{fc} is the L_2 regulation function, and ω is the parameters of its linear layer. Meanwhile, s is a hyper-parameter of the L_2 regulation function, which controls the strength of normalization. We will analyze the influences of β in the Section *Ablation Study*.

4 Experiments

Experimental Settings

Datasets. In our experiment, we used three distinct datasets, which are publicly available, to evaluate our method. All of these three datasets are related to the facial images. The summary of these datasets is presented in Table 1. Each dataset comprises real and fake images generated by the deep learning approaches. For instance, the real images of StarGAN (Choi et al. 2018) are provided by CelebA (Liu et al. 2015) while the fake images are developed by the StarGAN model. The real images of both StyleGANs (Karras, Laine, and Aila 2019; Karras et al. 2020) and StyleGAN2 are created by FFHQ (Karras, Laine, and Aila 2019), and the fake images of them are generated by the StyleGAN and StyleGAN2 respectively. The datasets are all balanced, which means the number of real images and the number of fake images are equal. We separated three parts of the dataset for the training, validation, and testing. The row in the table shows the data size in our experiment. In addition, we isolated 2000 images for each dataset to carry out the transfer learning process.

Baselines. In this section, we compare our method X-Transfer with two existing approaches. We chose the best

Dataset	StarGAN	StyleGAN	StyleGAN2
Resolution	128 × 128	256 × 256	256 × 256
Train	137,239	33,739	42,356
Test	50,000	30,000	30,000
Transfer	2000	2000	2000
Source	Real: CelebA Fake: StarGAN	Real: FFHQ Fake: StyleGAN	Real: FFHQ Fake: StyleGAN2

Table 1: An overview of datasets

practice for the comparison. In addition, we identified the optimized hyper-parameter settings in the ablation study; we carried out various experiments, including analyzing the effect of β , investigating the data augmentation, and generalizing our model on the non-face image dataset.

General-Transfer. The common way to perform transfer learning is by freezing some weights of a pre-trained model learned from the source dataset and fine-tuning it with weight decay for the target dataset. We experimented with this method for GAN image detection and called it General-Transfer. To clarify, we froze most of the convolutional layers except for the final convolutional block and linear layers.

The base model is RepVGG-A0, and General-Transfer was trained for 300 epochs in the transfer stage with a learning rate of 0.04 and momentum rate of 0.1. In addition, we employed different data augmentation methods such as RandomHorizontalFlip and Gaussian compression. At the same time, we also used SGD and cosine annealing algorithm (Loshchilov and Hutter 2016) to adjust learning rate decay dynamically. The training step can be terminated in advance when the learning rate drops to 0.

T-GD. In addition to general transfer, we conducted T-GD as our second baseline. This method is original from reference (Jeon et al. 2020). We modified the model and trained it for 300 epochs in the pre-train stage and at least 300 in the transfer stage. During the transfer stage, we utilized cut-mix (Yun et al. 2019) for data augmentation, which can improve the performance in detecting GAN images. T-GD uses L2 regularization to constrain the convolutional layer parameters' variation, thereby preserving the source dataset's performance during the transfer stage and preventing catastrophic forgetting.

In our experiment, we followed the same data augmentation and learning strategy as general transfer except for cut-mix. All the probability of data augmentation is 50%. In our method X-transfer, We employ the same experimental metric AUC and dataset except the PGGAN dataset as T-GD. We set the initial learning rate as 0.002 in the transfer stage, using low momentum by 0.001 for stochastic gradient descent (SGD) inspired by (Li et al. 2020). In addition, we have set JPEG data augmentation with random compression quality, which samples randomly from 30 to 100.

Base Architecture. In both the pre-train and transfer stages, we use the RepVGG-A0 network (Ding et al. 2021) as the binary classifier of our backbone because of its high accuracy and computational efficiency.

Evaluation Metric. We use the Area under the Receiver Op-

erating Characterization Curve(AUC) to evaluate the general performance of the model. Since the accuracy metric requires a fixed threshold to compute the effect of classification in advance, the AUC metric standard is more applicable than it is.

Results

General-Transfer vs X-Transfer. In the transfer stage, the General-Transfer method freezes the weights of the pre-trained model and fine-tunes it to learn from the target dataset. During this period, the General-Transfer presents a trade-off between the performance of the source and the target datasets. After transfer learning, we observed that General-Transfer achieved a higher AUC metric on either the source dataset or the lower one on the target dataset, but not necessarily both simultaneously. For instance, it may achieve a higher AUC on the source dataset but a lower one on the target dataset.

Our experimental results are depicted in table 2. In our test stage, when the transfer stage was from StarGAN to StyleGAN2, General-Transfer performed pretty well(91.1% in StarGAN and 95.7% in StyleGAN2). However, when the transfer was done from StyleGAN or StyleGAN2 to StarGAN, the performance of General-Transfer was poor, with accuracy levels reaching disaster proportions (99.4% in StarGAN and 59.8% in StyleGAN2).

On the contrary, X-Transfer shows more consistent performance on both the source and target datasets. It maintains the high performance achieved on the source dataset while transferring to the target dataset, resulting in impressive scores on both datasets.

T-GD vs X-Transfer. T-GD adopts an L2 regularization to limit the variation of layers’ parameters, which can maintain the performance on both the source and target datasets. Meanwhile, T-GD utilizes an adaptive iterative training method based on the teacher-student model, which can enhance the model’s ability to acquire knowledge better.

X-Transfer uses a sibling network to transport gradients in the order of corresponding blocks. Regarding experimental results, X-Transfer performs better on both the source and target datasets. When the model was trained by StarGAN and transferred to StyleGAN2, X-Transfer exhibited an advanced AUC metric(95.5%), whereas T-GD’s metric(90.01%) was slightly lower than X-Transfer.

Moreover, X-Transfer uses fewer epochs than T-GD in the process of transfer learning. In the transfer stage, T-GD spent at least 300 epochs, but X-Transfer only spent 10% of its epochs on average, both of which were trained with the same dataset. For instance, T-GD spent 300 epochs while transferring from StarGAN to StyleGAN2, but X-Transfer spent just 30 epochs during the transfer stage on the same dataset as T-GD.

With AUC Loss vs Without AUC Loss. We compare the difference between our method with and without the AUC Loss function when using the X-Transfer method. The primary target function combines binary cross-entropy, L2 regularization, and the AUC Loss function. As Table 2 shows above, no matter which dataset is utilized, at least one of

source dataset	target dataset	methods	source AUC	target AUC
StarGAN	StyleGAN2	General-Transfer	91.09%	95.70%
		T-GD	96.4%	90.1%
		X-Transfer	98.20%	90.21%
		X-Transfer + AUC Loss	99.04%	90.12%
StyleGAN2	StarGAN	General-Transfer	99.40%	59.80%
		T-GD	90.01%	90.0%
		X-Transfer	99.72%	92.30%
		X-Transfer + AUC Loss	99.90%	94.54%

Table 2: The results of transfer learning using AUC metric. We carried out an experiment to compare X-transfer (with or without AUC Loss) with the two baseline models, General-Transfer and T-GD. Each model is pre-trained on the source dataset and transferred to the target dataset. Here, we only show the results of StarGAN to StyleGAN2 and StyleGAN2 to StarGAN. The other transferring, e.g., StarGAN to StyleGAN or StyleGAN2, has been demonstrated in our Ablation study.)

the source or target datasets can achieve a higher performance than not using AUC Loss. With AUC Loss, the AUC on the target dataset is 2.24% higher than that without, and the score on the source dataset is 0.18% higher than without one. The experimental results also show that AUC Loss positively affects the transfer stage, regardless of whether it is applied to the source or target dataset.

Ablation Study

To identify the best practice settings for our comparison, we carried out several ablation experiments as follows:

Hyper-parameter Analysis for AUC. The selection of hyper-parameter $\beta \in [0, 1]$ can balance the binary cross-entropy(BCE) loss function and AUC loss function L_{AUC} as shown in Equation 6. We used different hyper-parameter β to evaluate the effect of AUC Loss. We trained our model with different β values. According to the results displayed in Figure 3, $\beta = 0.6$ yields the best detection performance while transferring StyleGAN2 to StarGAN.

Effect of Data Augmentation. Apart from the factors discussed above, we also investigated the impact of data augmentation in our experiment. We applied various data augmentation methods, such as Gaussian filtering, JPEG compression, and AlignMixup (Venkataramanan et al. 2022). The following table presents a detailed analysis of the impact of data augmentation in our experiments.

As depicted in Table 3, we investigated the impact of data augmentation on our X-Transfer method. Similarly, we used StarGAN as the pre-trained dataset and transferred it to StyleGAN as the target dataset. After applying data augmentation, the AUC score decreased from 98.94% to 97.42% on the target dataset. However, the score on the source dataset was still 5.56% higher than the score obtained without data augmentation, and the reduction of AUC on the target dataset(only 0.38%) didn’t affect much. Meanwhile, using data augmentation can expand the size of the dataset

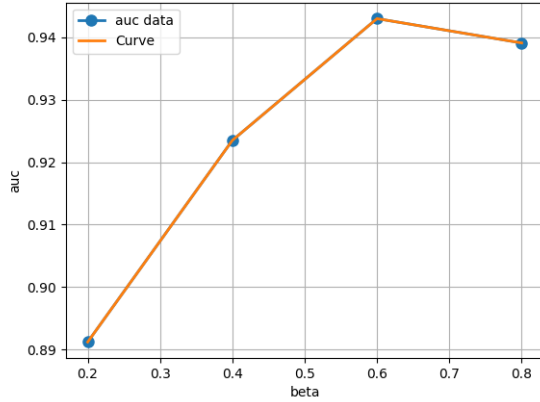


Figure 3: Impact of hyper-parameter β in AUC Loss in target dataset.

method	source dataset	target dataset	source AUC	target AUC
augmentaion	StarGAN	StyleGAN	98.82%	97.42%
no augmentation			93.16%	98.91%

Table 3: Impact of data augmentation in X-Transfer

and prevent the probability of over-fitting during the transfer stage.

Effect on Non-face Dataset. We also evaluated our method on non-face datasets, using two different types of datasets as the target dataset to validate the performance of our method. The non-face datasets include LSUN-Cat, LSUN-Church, and LSUN-Car (Yu et al. 2015). All the real datasets were obtained from the sources mentioned earlier (real ones from the CelebA and LSUN datasets and fake ones from StarGAN and StyleGAN2 generated from real ones). The source dataset was StarGAN, and the target dataset was a combination of the abovementioned datasets and StyleGAN2.

test dataset	Cat	Church	Horse
AUC	97.89%	98.12%	97.62%

Table 4: Impact on non-face dataset

All results are over 97% , and the best performance is using the LSUN-Church dataset, proving that our method can detect non-facial images effectively as well.

5 Conclusion

In this paper, we introduce a novel detection algorithm, X-Transfer, to detect GAN-generated images. Our method performs highly on the source and target datasets after the transfer learning phase. It combines using CNNs, data augmentation, transfer learning, and AUC Loss term. The main focus of our method is to preserve the performance of the source dataset without causing excessive forgetting of the

learned knowledge during transfer learning. We achieved it by utilizing two parallel neural networks propagating gradients through corresponding layers. Additionally, we incorporate the AUC Loss in our target loss terms as a reference, ensuring a higher AUC metric. This approach proves beneficial in training a high-performance detection model. Generative models’ intricate nature and rapid advancements present a formidable challenge in effectively identifying their generated images. A significant concern revolves around the scarcity of newly generated and the complexity of GAN images. To tackle this issue, the concept of few-shot or meta-learning shows promise, although it warrants further investigation. Numerous aspects await exploration by future researchers in this domain.

References

- Bayar, B.; and Stamm, M. C. 2016. A deep learning approach to universal image manipulation detection using a new convolutional layer. In *Proceedings of the 4th ACM workshop on information hiding and multimedia security*, 5–10.
- BURGESS, M. 2021. The Biggest Deepfake Abuse Site Is Growing in Disturbing Ways.
- Chen, B.; Ju, X.; Xiao, B.; Ding, W.; Zheng, Y.; and de Albuquerque, V. H. C. 2021. Locally GAN-generated face detection based on an improved Xception. *Information Sciences*, 572: 16–28.
- Choi, Y.; Choi, M.; Kim, M.; Ha, J.-W.; Kim, S.; and Choo, J. 2018. Stargan: Unified generative adversarial networks for multi-domain image-to-image translation. In *Proceedings of the IEEE conference on computer vision and pattern recognition*, 8789–8797.
- Cortes, C.; and Vapnik, V. 1995. Support-vector networks. *Machine learning*, 20: 273–297.
- Cox, D. R. 1958. The regression analysis of binary sequences. *Journal of the Royal Statistical Society Series B: Statistical Methodology*, 20(2): 215–232.
- Cozzolino, D.; Thies, J.; Rössler, A.; Riess, C.; Nießner, M.; and Verdoliva, L. 2018. Forensictransfer: Weakly-supervised domain adaptation for forgery detection. *arXiv preprint arXiv:1812.02510*.
- Ding, X.; Zhang, X.; Ma, N.; Han, J.; Ding, G.; and Sun, J. 2021. Repvgg: Making vgg-style convnets great again. In *Proceedings of the IEEE/CVF conference on computer vision and pattern recognition*, 13733–13742.
- Do, N.-T.; Na, I.-S.; and Kim, S.-H. 2018. Forensics face detection from GANs using convolutional neural network. *ISITC*, 2018: 376–379.
- Duda, R. O.; Hart, P. E.; et al. 1973. *Pattern classification and scene analysis*, volume 3. Wiley New York.
- Goodfellow, I.; Pouget-Abadie, J.; Mirza, M.; Xu, B.; Warde-Farley, D.; Ozair, S.; Courville, A.; and Bengio, Y. 2014. Generative Adversarial Nets. In *Neural Information Processing Systems*.
- He, K.; Zhang, X.; Ren, S.; and Sun, J. 2016. Deep Residual Learning for Image Recognition. *IEEE*.

- Jeon, H.; Bang, Y.; Kim, J.; and Woo, S. S. 2020. T-gd: Transferable gan-generated images detection framework. *arXiv preprint arXiv:2008.04115*.
- Karras, T.; Aila, T.; Laine, S.; and Lehtinen, J. 2017. Progressive growing of gans for improved quality, stability, and variation. *arXiv preprint arXiv:1710.10196*.
- Karras, T.; Laine, S.; and Aila, T. 2019. A style-based generator architecture for generative adversarial networks. In *Proceedings of the IEEE/CVF conference on computer vision and pattern recognition*, 4401–4410.
- Karras, T.; Laine, S.; Aittala, M.; Hellsten, J.; Lehtinen, J.; and Aila, T. 2020. Analyzing and improving the image quality of stylegan. In *Proceedings of the IEEE/CVF conference on computer vision and pattern recognition*, 8110–8119.
- Krizhevsky, A.; Sutskever, I.; and Hinton, G. 2012. ImageNet Classification with Deep Convolutional Neural Networks. *Advances in neural information processing systems*, 25(2).
- Li, H.; Chaudhari, P.; Yang, H.; Lam, M.; Ravichandran, A.; Bhotika, R.; and Soatto, S. 2020. Rethinking the Hyperparameters for Fine-tuning.
- Li, H.; Chen, H.; Li, B.; and Tan, S. 2018. Can forensic detectors identify gan generated images? In *2018 Asia-Pacific Signal and Information Processing Association Annual Summit and Conference (APSIPA ASC)*, 722–727. IEEE.
- Liu, Z.; Luo, P.; Wang, X.; and Tang, X. 2015. Deep Learning Face Attributes in the Wild. In *Proceedings of International Conference on Computer Vision (ICCV)*.
- Loshchilov, I.; and Hutter, F. 2016. Sgdr: Stochastic gradient descent with warm restarts. *arXiv preprint arXiv:1608.03983*.
- Mi, Z.; Jiang, X.; Sun, T.; and Xu, K. 2020. GAN-Generated Image Detection with Self-Attention Mechanism against GAN Generator Defect. *IEEE Journal of Selected Topics in Signal Processing*, PP(99): 1–1.
- Mo, H.; Chen, B.; and Luo, W. 2018a. Fake faces identification via convolutional neural network. In *Proceedings of the 6th ACM workshop on information hiding and multimedia security*, 43–47.
- Mo, H.; Chen, B.; and Luo, W. 2018b. Fake Faces Identification via Convolutional Neural Network. In *the 6th ACM Workshop*.
- Nataraj, L.; Mohammed, T. M.; Chandrasekaran, S.; Flenner, A.; Bappy, J. H.; Roy-Chowdhury, A. K.; and Manjunath, B. S. 2019. Detecting GAN generated Fake Images using Co-occurrence Matrices. *Electronic Imaging*.
- Simonyan, K.; and Zisserman, A. 2014. Very Deep Convolutional Networks for Large-Scale Image Recognition. *Computer Science*.
- Song, L.; Wu, J.; Yang, M.; Zhang, Q.; Li, Y.; and Yuan, J. 2021. Robust knowledge transfer via hybrid forward on the teacher-student model. In *Proceedings of the AAAI conference on Artificial Intelligence*, volume 35, 2558–2566.
- Venkataramanan, S.; Kijak, E.; Amsaleg, L.; and Avrithis, Y. 2022. Alignmixup: Improving representations by interpolating aligned features. In *Proceedings of the IEEE/CVF Conference on Computer Vision and Pattern Recognition*, 19174–19183.
- Wang, S. Y.; Wang, O.; Zhang, R.; Owens, A.; and Efros, A. A. 2020. CNN-Generated Images Are Surprisingly Easy to Spot... for Now. In *2020 IEEE/CVF Conference on Computer Vision and Pattern Recognition (CVPR)*.
- Yan, L.; Dodier, R. H.; Mozer, M.; and Wolniewicz, R. H. 2003. Optimizing classifier performance via an approximation to the Wilcoxon-Mann-Whitney statistic. In *Proceedings of the 20th international conference on machine learning (icml-03)*, 848–855.
- Yang, X.; Li, Y.; and Lyu, S. 2019. Exposing deep fakes using inconsistent head poses. In *ICASSP 2019-2019 IEEE International Conference on Acoustics, Speech and Signal Processing (ICASSP)*, 8261–8265. IEEE.
- Yu, F.; Zhang, Y.; Song, S.; Seff, A.; and Xiao, J. 2015. LSUN: Construction of a Large-scale Image Dataset using Deep Learning with Humans in the Loop. *computer science*.
- Yun, S.; Han, D.; Oh, S. J.; Chun, S.; Choe, J.; and Yoo, Y. 2019. Cutmix: Regularization strategy to train strong classifiers with localizable features. In *Proceedings of the IEEE/CVF international conference on computer vision*, 6023–6032.